The W.R. Wiley Environmental Molecular Sciences Laboratory (EMSL) is a U.S. Department of Energy (DOE) national scientific user facility located at Pacific Northwest National Laboratory (PNNL) in Richland, Washington. EMSL is operated by PNNL for the DOE Office of Biological and Environmental Research. At one location, EMSL offers a comprehensive array of leading-edge resources in six research facilities.

Access to the capabilities and instrumentation in EMSL facilities is obtained on a peer-reviewed proposal basis, and users are participants on accepted proposals. EMSL staff members work with users to expedite access to the research facilities, support capabilities, and the resident scientific expertise. The bimonthly report documents research and activities of EMSL staff and users.

Research Highlights

Reactive Ballistic Deposition of Porous TiO_2 Films: Growth and Characterization

DW Flaherty,[(a)] Z Dohnálek,[(b)] A Dohnálková,[(c)] BW Arey,[(c)] DE McCready,[(c)] P Nachimuthu,[(c)] CB Mullins,[(a)] and BD Kay[(b)]

(a) University of Texas at Austin, , Austin, Texas

(b) Pacific Northwest National Laboratory, Richland, Washington

(c) W.R. Wiley Environmental Molecular Sciences Laboratory, Richland, Washington

Titania (TiO_2) is widely used as a catalyst and may provide a pathway for the use of solar radiation as a viable source of clean energy. This work describes a method to create nanoporous TiO_2 films with a combination of high surface area and thermal stability that could serve as supports for applications in heterogeneous catalysis.

As a material, titania (TiO_2) has attracted much attention because of its uses in a wide range of applications such as heterogeneous catalysts, gas sensors, photocatalysts, optical coatings, and pigments. Correspondingly, it is the most studied metal oxide in surface science. Recently, there has been great interest in the growth and chemical characterization of metal-oxide-supported metal particles and thin films as model systems for industrial catalytic systems. These films are of interest from the aspect of fundamental chemistry and for the study of surfaces that better emulate those employed in industrial catalytic systems.

In this study, we explored high-surface-area, porous TiO_2 thin films grown using reactive ballistic deposition (RBD) and glancing angle deposition techniques. In prior work, we showed that these techniques can produce highly porous, high-surface-area metals, metal oxides, and other materials. The techniques are based on a simple shadowing model. At glancing angles, random height differences that arise during the initial film growth can block incoming flux, essentially creating shadows that result in void regions in the shadowed region. If surface and/or bulk diffusion are slow compared to the incident flux (i.e., if the molecules "hit and stick"), then the voids remain unfilled. Continued deposition results in porous films with filamentous columnar morphologies. Varying degrees of film porosity can be achieved by varying the deposition angle and substrate temperature.

Figure 1 shows scanning electron microscopy (SEM) images for a 750 ML thick TiO_2 film deposited 85° from substrate normal and at a sample temperature of 300 K. The images confirm that the film consists of an array of separated filaments that grow toward the physical vapor deposition source. Figure 1C shows a film deposited at 85° and 100 K; the image of this film appears to be very similar to the film grown at 300 K. The images indicate that an increase in temperature from 100 to 300 K does not increase the mobility of ad-atoms enough to affect the morphology of the film. Figure 1D is a SEM image of a film deposited at 70° and 300 K. Decreasing the deposition angle from 85° to 70° has a dramatic effect on film structure as seen in

Figure 1D. On this length scale, a film deposited at 70° appears dense, but films deposited at this angle actually prove to have the greatest surface area as was confirmed using nitrogen adsorption.

Transmission electron microscopy (TEM) of filaments scraped from the tantalum plate and placed on amorphous carbon grids was performed. The filaments grown at both 100 and 300 K reveal nanoscale features within the filaments when viewed under high magnification (Figure 2A). Selected area diffraction (SAD) analysis of individual filaments indicates that the filaments are predominantly amorphous; however, in some cases randomly oriented groups of filaments display the well-defined diffraction patterns seen in insets (B) and (C) of Figure 2. D-spacing values extracted from these SAD patterns are indicative of the rutile phase.

This work confirms that nanoporous, high-surface area films of TiO_2 can be synthesized by reactive ballistic deposition of titanium metal in under oxygen ambient conditions. The SEM and TEM results show that the films consist of arrays of separated filaments. The surface area and the distribution of binding site energies of the films were measured as functions of growth temperature, deposition angle, and annealing conditions using temperature programmed desorption of nitrogen. We found that TiO_2 films deposited at 70° and 50 K exhibited the greatest specific surface area (i.e., 100 m^2/g). In addition, the films retain greater than 70 percent of their original surface area after annealing to 600 K. The combination of high surface area and thermal stability suggests that these films could serve as supports for applications in heterogeneous catalysis. This exciting work was recently published in the *Journal of Physical Chemistry C*.

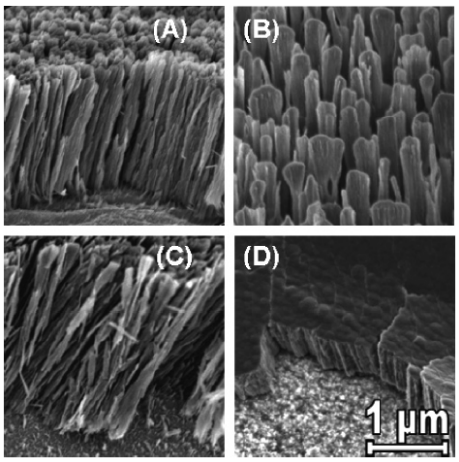

Figure 1. SEM images of TiO_2 films deposited via RBD. (A) Top and (B) side views of a film grown at 300 K and at a deposition angle of 85°. (C) Side view of a film grown at 100 K and 85°, (similar in appearance to the film grown at 300 K). (D) Side view of a film grown at 300 K and at 70°.

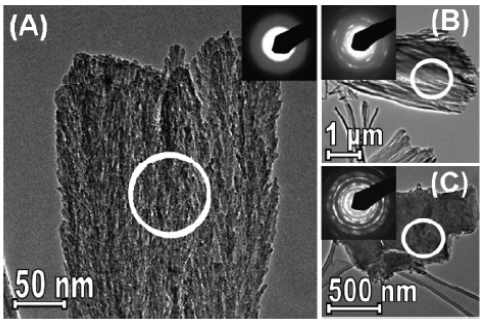

Figure 2. TEM images of TiO_2 films accompanied by insets with SAD. (A) A single amorphous filament from a film deposited at 85° and 300 K. (B) A cluster of filaments from the same film as (A) displaying a SAC pattern corresponding to polycrystalline rutile TiO_2. (C) A portion of a film grown at 70° and 300 K with a high degree of crystallinity.

Citation

Flaherty, DW, Z Dohnálek, A Dohnálkova, BW Arey,DE McCready, N Ponnusamy, CB Mullins, and BD Kay. 2007. "Reactive Ballistic Deposition of Porous TiO_2 Films: Growth and Characterization." *Journal of Physical Chemistry C* 111(12):4765-4773. Available at http://pubs.acs.org/cgi-bin/article.cgi/jpccck/2007/111/i12/html/jp067641m.html

Specific Bonds between Iron Oxide Surface and Outer Membrane Cytochromes MtrC and OmcA from *Shewanella oneidensis* MR-1

BH Lower,[(a)] L Shi,[(a)] R Yongsunthon,[(b)] TC Droubay,[(a)] DE McCready,[(c)] and SK Lower[(b)]

(a) Pacific Northwest National Laboratory, Richland, Washington
(b) Ohio State University, Columbus, Ohio
(c) W.R. Wiley Environmental Molecular Sciences Laboratory, Richland, Washington

In this study, we used atomic force microscopy to show that membrane cytochromes MtrC and OmcA purified from Shewanella oneidensis MR-1are able to form a stable bond with the surface of the iron oxide hematite (Fe_2O_3).

Dissimilatory iron-reducing microorganisms (DIRMs) have evolved the ability to reduce iron oxide minerals, thereby coupling Fe(III) reduction to the oxidation of energy-rich carbon compounds. The mechanism of dissimilatory iron reduction is not known because of the complexity of the biogeochemical reactions that occur at the mineral-microbe interface. Because most iron oxides exist as solids in the environment (e.g., hematite), particular challenges exist for DIRMs with regard to transferring electrons from inside the cell where they are generated, across the cellular membrane, and then to the exterior of the cell where the Fe(III) in iron oxides serves as the terminal electron acceptor. *S. oneidensis* MR-1 is a DIRM that is purported to use the outer membrane cytochromes MtrC and OmcA to catalyze the transfer of electrons directly to Fe(III) in iron-bearing minerals during anaerobic respiration. A prerequisite for this type of reaction is the formation of a stable bond between the cytochrome and the iron oxide surface.

In our study, the force spectra obtained between pure cytochromes and Fe_2O_3 exhibited a strong correlation with those obtained between living *S. oneidensis* MR-1 cells and Fe_2O_3. This finding is shown in Figure 1, which compares force spectra obtained between MtrC-hematite (blue), OmcA-hematite (red), and *S. oneidensis* MR-1-hematite (green). These results suggest that *S. oneidensis* MR-1 expresses MtrC and OmcA on the cell surface where the cytochromes make direct contact with an iron oxide surface and play a prominent role in the terminal electron transfer reaction that occurs between *S. oneidensis* MR-1 and a Fe(III)-bearing mineral during anaerobic respiration. Figure 2 is a schematic showing the proposed mechanism of dissimilatory Fe(III) reduction in *S. oneidensis* MR-1.

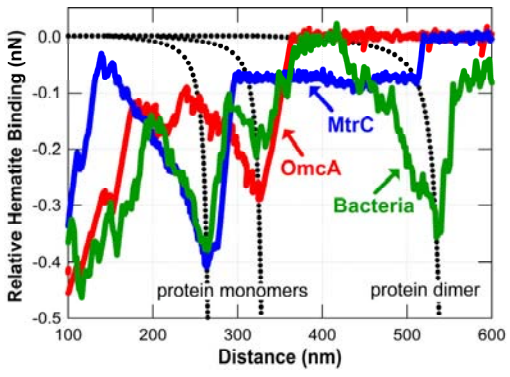

Figure 1. Comparison of force spectra obtained between MtrC-hematite (blue), OmcA-hematite (red), and *S. oneidensis* MR-1-hematite (green).

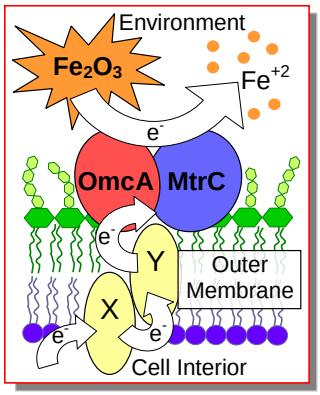

Figure 2. Schematic showing the proposed mechanism of dissimilatory Fe(III) reduction in *S. oneidensis* MR-1.

Citation

Lower BH, L Shi, R Yongsunthon, TC Droubay, DE McCready, and SK Lower. 2007. "Specific Bonds between an Iron Oxide Surface and Outer Membrane Cytochromes MtrC and OmcA from *Shewanella oneidensis* MR-1." *Journal of Bacteriology 189*: In press.

Structural Studies of Apo NosL, an Accessory Protein of the Nitrous Oxide Reductase System

LM Taubner,[(a)] MA McGuirl,[(b)] DM Dooley,[(a)] and V Copié[(a)]

(a) Montana State University, Bozeman, Montana
(b) University of Montana, Missoula, Montana

In this project, the researchers are seeking an understanding of proteins important for cleaning up groundwater, soils, and wetlands that have been contaminated by fertilizer run-off.

Denitrification, the process of reducing nitrate and nitrite to nitrogen gas, occurs under anaerobic conditions in both terrestrial and marine ecosystems. NosL is a 20-kDa copper binding lipo-protein needed for nitrous oxide reductase (N_2OR) assembly in denitrifying bacteria. This lipo-protein was discovered to have a very unique structure with a new configuration to bind and transport metal atoms in cells.

N_2OR performs the last step of denitrification, the conversion of nitrous oxide to dinitrogen (N_2), thus cycling nitrogen derived from biomass back to the atmosphere. To accomplish this energetically demanding reaction, N_2OR uses two functionally critical multi-nuclear copper clusters: 1) an electron donor site, Cu_A, and 2) a catalytic site, Cu_Z. Formation of this catalytic complex requires copper and sulfur, both of which can be toxic to the organism, thus necessitating dedicated uptake and transport systems to prevent undesirable side reactions and to ensure safe delivery of these species to the appropriate targets. The nosDFYL operon, located downstream of the N_2OR structural gene, nosZ, has been implicated in Cu_Z biogenesis. One gene in this operon, the nosL gene, is present in all denitrifying genomes sequenced thus far, suggesting an important function for this protein in N_2OR maturation. NosL has little sequence similarity with proteins that have a known function; therefore, the sequence reveals little about the NosL role in N_2OR assembly. NosL is known to bind copper and release it upon oxidation, so it likely functions as a metallochaperone to facilitate copper transport.

This research was led by V Copié of Montana State University with consultation from staff of the EMSL High-Field Magnetic Resonance Facility. Vital high-field nuclear magnetic resonance data (i.e., obtained at 800 MHz) enabled protein structure determination on the apo nosL protein (with no copper bound to the protein). The structure was discovered to consist of two flat planes connected by a short loop, with the planes oriented perpendicular to each other. As can be seen in Figure 1, each plane contains a ββαβ structure. Both the ββαβ structure and the planes oriented perpendicular to each other with a large cleft between them are unique structural motifs in NosL. Another surprising feature is that although the two planes have very different sequences, they have nearly identical structures. Only one other protein found in the protein data bank has a similar structure, the MerB protein, which is an organomercury lyase involved in a bacterial mercury resistance system. In the case of NosL and MerB, this conserved mechanistic feature would appear to require the presence of a large cleft between the two ββαβ domains contiguous with a mononuclear metal-binding site. NosL has the same highly conserved methionine in the cleft, which is likely to be involved in binding the copper ion. The most likely function for this protein is to chaperone copper atoms through the cell and deliver it to N_2OR for incorporation into the enzyme. Supporting experiments indicate the protein binds Cu(I) and then releases it upon oxidation.

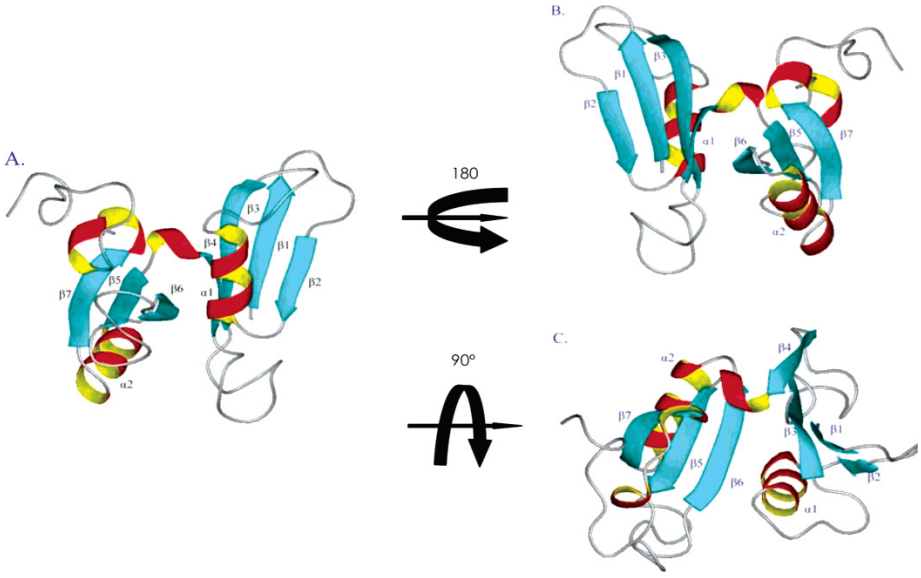

Figure 1. Ribbon diagrams of a representative low-energy conformer of apo NosL viewed from various orientations: (A) The ß sheets are depicted in cyan, helices in red and yellow; (B) A view of the apo NosL structure rotated by 180° relative to the orientation in panel A; (C) The image rotated 90° relative to the orientation in panel A illustrates the perpendicular relationship of the two ß sheets.

This structural work, published in the journal *Biochemistry* (Taubner et al. 2006), yielded the first detailed structure of an accessory protein from the nos cluster. It establishes the groundwork for understanding the role of the NosL protein in the bacterial N_2OR complex denitrification system.

Citation

Taubner LM, MA McGuirl, DM Dooley, and V Copié. 2006. "Structural Studies of Apo Nosl, an Accessory Protein of the Nitrous Oxide Reductase System: Insights from Structural Homology with MerB, a Mercury Resistance Protein." *Biochemistry* 45(40):12240-12252.

Proteomic Comparison between Virulent and Avirulent *Burkholderia mallei* Strains

SE Schutzer,[(a)] D DeShazer,[(b)] SO Purvine,[(c)] JE Turse,[(d)] AA Schepmoes,[(d)] and MS Lipton[(d)]

(a) University of Medicine and Dentistry of New Jersey, Newark, New Jersey
(b) U.S. Army Medical Research Institute of Infectious Diseases, Fort Detrick, Maryland
(c) W.R. Wiley Environmental Molecular Sciences Laboratory, Richland, Washington
(d) Pacific Northwest National Laboratory, Richland, Washington

The bacterium Burkholderia mallei can cause severe human illness and has been classified by the Centers for Disease Control and Prevention as a category B agent in the list of potential bioterrorism agents. Differentiating between virulent and avirulent B. mallei strains is difficult, which complicates subsequent treatment and threat assessment. This work is using EMSL's high-throughput proteomics capabilities to compare the virulent and avirulent strains to reveal information as to the source of virulence.

Although most of the 30 species of *Burkholderia* bacteria are saprophytes or plant pathogens, two species pose a significant threat to animal and human health. One species, *B. pseudomallei*, the causative agent for the infectious disease melliodosis, affects populations throughout Southeast Asia and Australia. The other species, *B. mallei*, is primarily an animal pathogen and is the causative agent of the disease known as glanders.

This worldwide disease poses a significant health threat to cystic fibrosis patients and immunocompromised individuals, and is considered a potential biowarfare agent (Huelseweh et al. 2006). While several avirulent strains of *B. mallei* are known to exist, the source of attenuation is not. Currently, there is no rapid discriminating diagnostic assay, vaccine, or reliable therapy for *B. mallei*; high DNA homology severely limits the ability to distinguish avirulent and virulent strains by standard molecular biology techniques.

We hypothesize that several virulence factors account for the differential pathogenicity of *B. mallei* strains. To test this hypothesis, we are using a high-throughput liquid chromatography-mass spectrometry-based approach (Hixson et al. 2006; Zimmer et al. 2006) to compare proteins expressed in the virulent ATCC 23344 strain with those expressed by the nonvirulent NCTC 10247 strain and to identify differences in protein expression and abundance under identical *in vitro* growth conditions. The genome of *B. mallei* ATCC 23344 has been fully sequenced and known to contain several common virulence factors, including a type-III secretion system, lipopolysaccharide (LPS)-biosynthesis genes, iron-response genes, quorum-sensing elements, integration host factor (*ihf*A and *ihf*B), and genes that respond to reactive oxygen or nitrogen intermediates.

Using this approach, we detected and quantified 751 proteins, from which 126 exhibited a twofold abundance difference ($p \leq 0.05$) between the avirulent and virulent strains (Figure 1). Thirty-one unique proteins were observed in the virulent ATCC 23344 strain, and of these, three proteins— 1) integration host factor B, 2) ferredoxin (Rivera-Marrero et al. 1998), and 3) the chemotaxis protein CheZ (Lee et al. 2001)—have properties identified as virulence factors in other systems. Additionally, the LPS biosynthesis proteins were fivefold more abundant in the virulent strain. Analysis of the avirulent NCTC 10247 strain revealed 135 uniquely expressed proteins, of which more than 10 percent have annotations as conserved hypothetical genes (i.e., no known functions) and are ideal targets for further genetic and molecular biological assays.

Although this work has just recently begun, peptides examined from a global preparation of *Burkholderia* grown *in vitro* have already revealed key differences in protein expression between strains of *B. mallei*. Remaining work will examine peptides from the cytoplasm and membrane components of these two strains.

Figure 1. Relative abundance data plot for 751 proteins from *B. mallei* global proteome digestion, triplicate analysis. Mass spectrometry intensity values were normalized to ribosomal protein abundances, avirulent strain NCTC 10247 was used as the baseline comparator. Results show significant differences between the virulent and avirulent strains, which may lead to further discovery or development of clinical biomarkers.

Citations

Hixson KK, JN Adkins, SE Baker, RJ Moore, BA Chromy, RD Smith, SL Mc-Cutchen-Maloney and MS Lipton. 2006. "Biomarker Candidate Identification in *Yersinia pestis* using Organism-Wide Semiquantitative Proteomics." *Journal of Proteome Research* 5(11):3008-3017.

Huelseweh B, R Ehricht, H-J Marschall. 2006. "A Simple and Rapid Protein Array Based Method for the Simultaneous Detection of Biowarfare Agents." *Proteomics* 6(10):2972-2981.

Lee SH, SM Butler, A Camilli. 2001. "Selection for *In Vivo* Regulators of Bacterial Virulence." *Proceedings of the Nationall Academy of Sciences USA* 98(12):6889-6894.

Rivera-Marrero CA, MA Burroughs, RA Masse, FO Vannberg, DL Leimbach, J Roman and JJ Murtagh. 1998. "Identification of Genes Differentially Expressed in *Mycobacterium tuberculosis* by Differential Display PCR." *Microbial Pathology* 25(6):307-316.

Zimmer JS, ME Monroe, WJ Qian and RD Smith. 2006. "Advances in Proteomics Data Analysis and Display Using an Accurate Mass and Time Tag Approach." *Mass Spectrometry Review* 25(3):450-482.

De Novo Structure-Based Molecular Design

BP Hay[(a)] and VS Bryantsev[(a)]

(a) Pacific Northwest National Laboratory, Richland, Washington

An important theme in supra-molecular chemistry is the formation of anion complexes using synthetic host molecules; however, identification of suitable hosts is not a trivial task. To address this issue, we have developed the de novo structure-based design software, HostDesigner, which is specifically tailored to discover molecular structures that are organized to complex with small guest molecules.

In a previous study, we identified bis-urea podands that are structurally organized for binding tetrahedral oxyanions (Bryantsev and Hay 2006). However, whether 1) any of the candidates will exhibit a significant steric preference for a tetrahedral guest or 2) some of the candidates will accommodate other anion shapes with equal facility remained to be determined. The current study represents the first step in an effort to explore the possibility of achieving anion shape selectivity—that is, the design of bis-urea tweezers that are structurally organized for binding tetrahedral ClO_4^-, trigonal NO_3^-, and spherical Cl^- anions.

Bis-urea host molecules were constructed using the *de novo* structure-based design software, HostDesigner, as described previously by Bryantsev and Hay (2006). Structures were built by connecting two N-methylurea-anion (nitrate and chloride) fragments with a hydrocarbon fragment taken from the library. Subsequent molecular mechanics analysis was applied to provide a more accurate prioritization of the top candidates. The top 500 candidates from each run are placed in order of increasing the relative binding energy, ΔG_{rel} to yield the final candidate ranking. The following expression was used to determine the ordering of relative binding energies:

$$\Delta G_{rel} = \Delta E_1 + \Delta E_2 + 0.31 x N_{rot},$$

where ΔE_1 = E(binding form) – E(global minimum), ΔE_2 = E(complex) – E(host, binding form) – E(guest), and N_{rot} is the number of freely rotating bonds restricted on complexation.

The results revealed that many bis-urea podands complementary for one anion shape can also accommodate other anion shapes. This finding is not surprising because the optimal placements for two urea groups around the spherical Cl^-, trigonal planar NO_3^-, and tetrahedral ClO_4^- are similar (Figure 1) (Hay et al. 2005), and if the host is flexible enough, it can easily adopt a conformation suitable for a particular anion geometry.

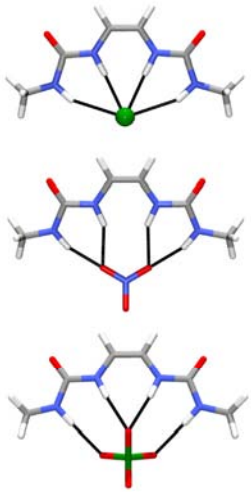

Figure 1. Geometries obtained for complexes of one candidate architecture with Cl^-, NO_3^-, and ClO_4^- reveal that this host can form four hydrogen bonds with all three anion shapes.

Citations

Bryantsev VS and BP Hay. 2006. "*De Novo* Structure-Based Design of Bisurea Hosts for Tetrahedral Oxdoanion Guests." *Journal of the American Chemical Society* 128(6):2035-2042.

Hay BP, TK Firman, and BA Moyer. 2005. "Recognition through the Complementary Placement of Urea Donor Groups." *Journal of the American Chemical Society* 127(6): 1810-1819.

Epitaxial Growth and Microstructure of Cu_2O Quantum Dots/Thin Films on $SrTiO_3$(100)

ZQ Yu,[(a)] CM Wang,[(b)] MH Engelhard,[(b)] P Nachimuthu,[(b)] DE McCready,[(b)] IV Lyubinetsky,[(b)] and S. Thevuthasan[(b)]

(a) Nanjing Normal University, Nanjing, China

(b) Pacific Northwest National Laboratory, Richland, Washington

Cuprous oxide (Cu_2O) is a non-stoichoimetric p-type semiconductor that shows unique electronic structure for applications related, in particular, to chemical and photochemical process such as water splitting under visible light irradiation. Finding an appropriate substrate, such as $SrTiO_3$ (STO), on which Cu_2O thin-film/quantum dots could be grown would help form hetero-junctions and effectively separate electron-hole pairs, thereby enhancing energy conversion efficiency.

In this paper, we report the epitaxial growth of Cu_2O thin films on an STO(100) surface. In the EMSL ultrahigh vacuum (UHV) chamber, the substrates were cleaned using oxygen plasma (1.0×10^{-5} torr oxygen partial pressure, 200-W power level) with a sample temperature of 600°C. During growth, Cu was evaporated from an effusion cell in the presence of the oxygen plasma while the substrate was kept at a temperature between 450 and 850°C. The growth rate of the film was controlled by changing the Cu flux, which was monitored by a quartz-crystal oscillator. The growth of the island (specimen A) and film (specimen B) could be obtained at Cu fluxes of 6×10^{-4} nm/s and1×10^{-3} nm/s, respectively.

Films grown under the two growth rates were similarly dominated by the Cu_2O phase, which showed a preferred orientation with respect to the substrate such that Cu_2O (200)//STO(100) as shown in Figure 1. The core-level Cu 2p x-ray photoelectron spectroscopy (XPS) image of sample A is shown in Figure 2(a). This image indicates that for sample A, the Cu at the very top layer possesses a valence state of +2. After removing approximately 5 nm from the very top layer by sputtering, the Cu^{2+} peak disappears, and instead, as illustrated in Figure 1(a), the Cu^{+} dominates. Cu 2P3/2 and 2P1/2 XPS spectra of sample B for the as-deposited case and after sputtering to remove a surface layer of approximately 5 nm are shown in Figure 2(b). The main peaks of Cu 2P3/2 and 2P1/2 lie at 931.8 and 952.0 eV, demonstrating that Cu in sample B exists only as Cu^{+}. This finding is consistent with the x-ray diffraction (XRD) results, which show a single Cu_2O phase.

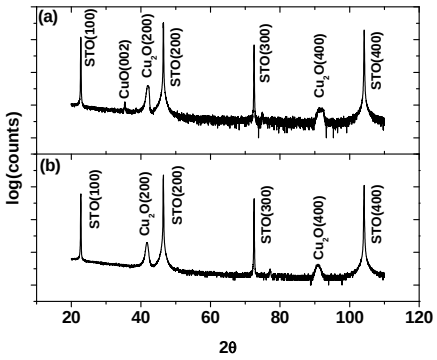

Figure 1. X-ray diffraction spectra of the samples.

Figure 3(a) is an atomic force microscopy (AFM) image of sample A that reveals a very rough surface. The rough surface was morphologically featured by the development of pyramids. The faces and edges of these pyramids are aligned, which indicates a similar crystallographic orientation of all the pyramids relative to the underline STO substrate. The insets shown in Figure 3(a) are two typical Wulff shape constructions of these pyramids. The transmission electron microscopy (TEM) image reveals that the pyramid has a typical height of approximately 200 nm, and all the pyramids are crystallographically aligned along the same direction with respect to the substrate. This point is clearly demonstrated by the selected area electron diffraction pattern shown in Figure 3(c). The overall orientation relationship between the substrate and the pyramid can be written as Cu_2O[001]//STO[001] and Cu_2O(1000//STO(100). This orientation relationship corresponds to a cube-on-cube orientation relationship between the cubic structured Cu_2O and STO. The computed diffraction pattern shown in Figure 3(d) consistently supports this finding.

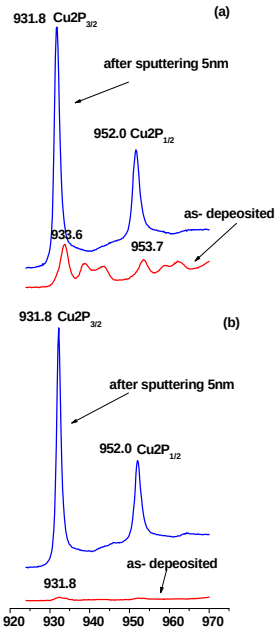

Figure 2. XPS spectra of the samples.

When compared with sample A, sample B shows a relatively flat surface as is shown in Figure 4(a). Careful scrutiny of the AFM image of sample B reveals that the surface of sample B also consists of very small pyramids, indicating a tendency for faceting of the film surface with the {111} planes. The cross-sectional TEM image shown in Figure 4(b) reveals that sample B indeed indicates growth of a Cu_2O thin film on the STO(100) surface. Both XRD and selected area electron diffraction revealed that, similar to the case of sample A, the thin film in sample B also possesses an epitaxial orientation relationship with the substrate: Cu_2O[001]//STO[001] and Cu_2O (1000//STO(100). This orientation is demonstrated by the electron diffraction patterns shown in Fig. 4(c) and Fig. 4(d).

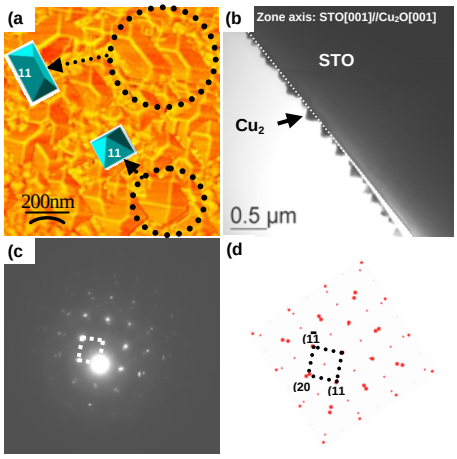

Figure 3. (a) AFM image, (b) TEM image, (c) electron diffraction pattern, and (d) calculated electron diffraction pattern.

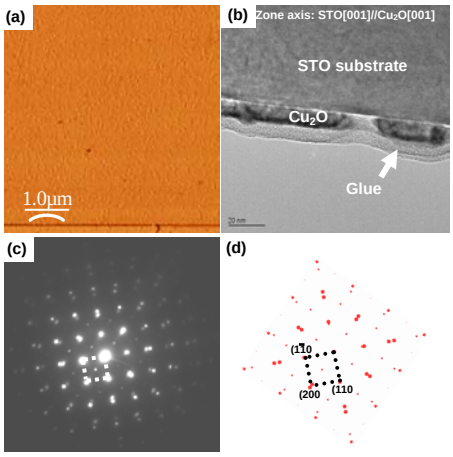

Figure 4. (a) AFM Image, (b) TEM image, (c) electron diffraction pattern, and (d) calculated electron diffraction pattern.

The dramatic difference in the morphology of specimen A and specimen B can be examined from the perspective of growth kinetics. For the case of a fast growth (e.g., for sample B), the growth rate is high; therefore, it leaves the system only a relatively short time to reach a configuration by which the overall energy of the system is minimized. On the other hand, in the case of low growth, the atoms will migrate, thereby allowing the system to develop a configuration by which the overall energy of the whole system will be minimized. Typically, development of a pyramid structure confined by the {111} planes is energetically more favored than development of a flat surface that is dominated by a $Cu_2O(100)$-type plane. Energetically, we would expect high-temperature annealing of a Cu_2O thin film, such as that developed in sample B, to promote formation of pyramid-structured quantum dots as shown in the microstructure developed in sample A.

Direct Observation of Adsorption Evolution and Bonding Configuration of TMAA on TiO_2(110)

I Lyubinetsky,[(a)] ZQ Yu,[(b)] and MA Henderson[(a)]

(a) Pacific Northwest National Laboratory, Richland, Washington

(b) Nanjing Normal University, Nanjing, China

Trimethyl acetic acid (TMAA) adsorption evolution on the rutile TiO2(110) surface from submonolayer-to-saturation coverages was examined at the atomic level by scanning tunneling microscopy. Upon TMAA deprotonation, no evidence of proton adsorbs on an adjacent bridging O^{2-} site has been found. It has been suggested that uncommon proton bonding configuration is favored instead. Such a configuration is likely to be stabilized by adjacent adsorbed carboxylate (TMA) groups.

The chemical interaction of molecules with titania (TiO_2) surfaces is crucial in a number of important fields, including catalysis and photocatalysis (Diebold 2003). Consistent with the known chemistry of organic acids on titania, TMAA adsorbs dissociatively on TiO_2(110) by O-H bond cleavage at or below 300 K. The TMA bridge-bonds across two Ti^{4+} cations, with the molecular plane oriented normal to the surface and along the Ti rows (the <001> direction). A highly ordered (2×1) TMA monolayer is formed at saturation coverage (Henderson et al. 2003; Onishi 2003). While it has been implicitly assumed that the acid proton adsorbs on

an adjacent bridging O^{2-} site, forming an OH^- group (Onishi 2003), there is no unambiguous evidence in the literature for the presence of these hydroxyl species.

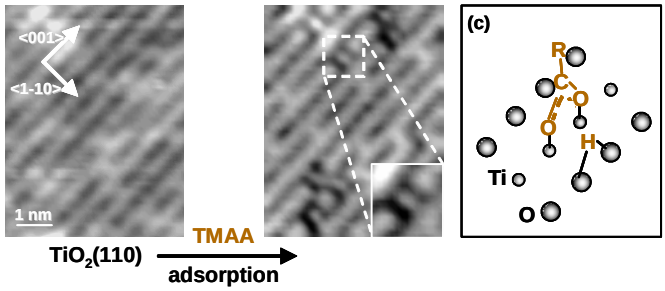

Figure 1. STM images of the same (5.5×7.5) nm^2 area: (a) before and (b) after TMAA exposure (coverage approximately 0.05 ML). The inset is a magnified view of one feature. Image (c) is a schematic model of the proposed proton bonding configuration.

Sequences of scanning tunneling microscopy (STM) images showing the same surface area with increasing adsorbate coverages have been acquired for the 260-300 K range (Lyubinetsky et al. 2007). Analysis of the same region during progressive adsorption allows us to monitor changes caused by the adsorption of single TMAA molecules Lyubinetsky et al. 1998). Figure 1 presents the same area images before and after a low-dose TMAA exposure. The adsorbed TMA species appear as a localized dark square-shaped feature with a bright protrusion in the middle. The TMA footprint covers just two neighboring Ti^{4+} atoms, giving additional, direct evidence for the bridge bonded TMA configuration discussed in literature (Onishi 2003). However, there is no indication of the appearance of OH^- groups in Figure 1b. Because proton abstraction is improbable based on temperature programmed desorption (TPD) results (White et al. 2004), we suggest that the deposited H atom takes on a different bonding configuration, with the proton attaching to a pair of bridging O atoms instead of to a single O atom. Certainly, considering the distance between two O atoms of 0.298 nm, the OH bond in the proton oxygen bridging configuration would be a relatively weak (in the terms of the hydrogen bond strength classification scheme) (Novak 1974). In addition, such a configuration may be stabilized by the proximity of the (negatively charged) TMA group adsorbed symmetrically on adjacent Ti^{4+} sites, as schematically shown in Figure 1c.

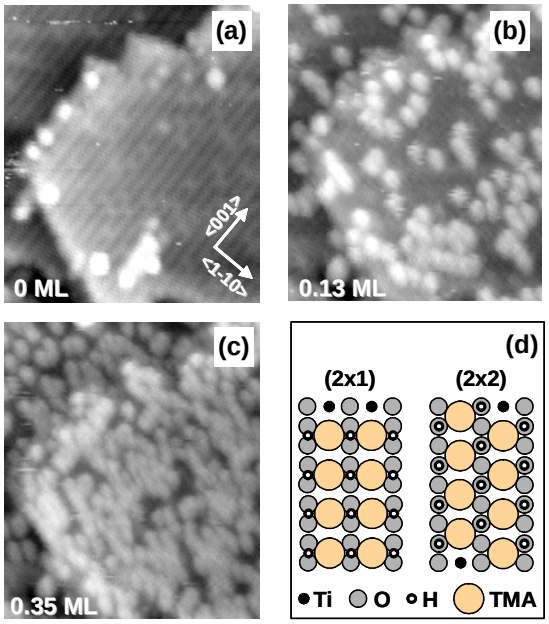

Figure 2. STM images of the same (16×20) nm^2 area of the TiO_2(110) surface (a) before and after adsorption of 0.13 ML (b), and 0.35 ML (c). Structural models of the TMA monolayer (image [d]) illustrate the favorable (2×1) TMA ordering (left model) by the suggested H bridging a pair of O sites. Alternative atop H attachment to single O ion would rather induce (2×2) ordering (right model).

Figure 2 illustrates an evolution of the TMAA adsorption throughout its consecutive stages by presenting the STM image snapshots of the same surface region starting from clean TiO_2(110) up to close to saturation of the monolayer. In the image before adsorption (Figure 2a), examples of bridging oxygen vacancies and also of a minor number of OH^- groups are differentiated by their relative contrast (Brookes et al. 2001; Wendt et al. 2005). After dosing with TMAA, the new features that appeared were relatively large bright spots centered on the Ti^{4+} rows (Figure 2b). These features are attributed to the TMA species bridge-bonding to two Ti^{4+} cations as a result of TMAA dissociation through deprotonation (Onishi 2003). (The appearance of TMA groups has changed when compared with the images shown in Figure 1, presumably because of changed STM tip apex conditions). Beginning from approximately 0.1 to 0.15 ML coverages, pairing along the <1-10> direction starts to form, while TMA groups tend to be separated along the Ti rows (<001> direction). This correlates with the tendency of carboxylates to repel each other along the <001> direction (Onishi 2003). Because no

significant surface diffusion of TMA has been observed in the studied temperature range, ordering in the <1-10> direction indicates the probable existence of a mobile precursor state. As coverage increases to 0.2 to 0.4 ML, TMA groups are forced to begin accommodating each other on adjacent Ti sites along the <001> direction, as is shown in Figure 2c. Eventually, a (2x1) TMA monolayer develops at nominal saturation coverage of 0.5 ML. Ordering of the TMA groups is possibly assisted by protons bridging between two oxygen sites, which effectively aligns adjacent carboxylates (Onishi 2003). As illustrated in the (2x1) structural model (left part of Figure 2d), such proton bonding is fully symmetric relative to adjacent TMA groups, and they would align the repulsive π-clouds of carboxylates through an electrostatic link by the adjacent protons. Alternative proton bonding (atop single O^{2-} ion) would be less symmetric and provide no apparent explanation for the (2x1) TMA ordering. Should atop proton bonding be present, it would rather favor a (2x2)- or (2xn)-type ordering based solely on a symmetry arguments. In this case, TMA groups would be shifted by a half-unit cell in the <001> direction in every second row in the (2x2) reconstruction, as shown in Figure 2d (right model) for one of the several possible OH configurations.

In summary, TMAA adsorption evolution on the TiO_2(110) surface from submonolayer to saturation coverages was examined at the atomic level by STM using the same area analysis approach. Upon TMAA deprotonation, no evidence of terminal OH group formation has been found. It has been suggested that uncommon geometry associated with a detached hydrogen atom takes place instead, with proton bonding to pair bridging oxygen atoms. Such a configuration is likely to be stabilized by adjacent adsorbed TMA groups and, in turn, be a factor in the formation of TMA (2x1) reconstruction at saturation coverage.

Citations

Diebold U. 2003. "The Surface Science of Titanium Dioxide." *Surface Science* 48(58):53-229.

Henderson MA, JM White, H Uetsuka, and H Onishi H. 2003. "Photochemical Charge Transfer and Trapping at the Interface between an Organic Adlayer and an Oxide Semiconductor." *Journal of the American Chemical Society* 125(49):14974-1495.

Onishi H. 2003. "Carboxylates Adsorbed on TiO_2." In *Chemistry of Nanomolecular Systems,* Springer Series in Chemical Physics 70, ed. T Nakamura, pp. 75-90, Springer, Berlin.

Lyubinetsky I, Z Dohnálek, WJ Choyke, and JT Yates. 1998. "Cl_2 Dissociation on Si(100)-(2x1): A Statistical Study by Scanning Tunneling Microscopy." *Physical Review B* 58(12): 7950-7957.

Lyubinetsky I, ZQ Yu, and MA Henderson. 2007. "Direct Observation of Adsorption Evolution and Bonding Configuration of TMAA on TiO_2(110)." *Journal of Physical Chemistry C* 111(11):4342-4346.

White JM, J Szanyi, and MA Henderson. 2004. "Thermal Chemistry of Trimethyl Acetic Acid on TiO_2(110)." *Journal of Physical Chemistry B* 108(11):3592-3602.

Novak A. 1974. "Hydrogen Bonding in Solids." In *Structure and Bonding*, Vol. 18, ed. JD Dunitz, pp. 177-216, Springer-Verlag, New York.

Brookes IM, CA Muryn, and G Thornton. 2001. "Imaging Water Dissociation on TiO_2(110)." *Physical Review Letters* 87(26): Article Number 266103.

Wendt S, R Schaub, J Matthiesen, EK Vestergaard, E Wahlstrom, MD Rasmussen, P Thostrup, LM Molina, E Laegsgaard, I Stensgaard, B Hammer, and F Besenbacher. 2005. "Oxygen Vacancies on TiO_2(110) and Their Interaction with H_2O and O_2: A Combined High-Resolution STM and DFT Study." *Surface Science* 5989(1-3):226-245.

Scientific Grand Challenge Highlights

High-Performance Sequence Analysis for Data-Intensive Bioinformatics

CS Oehmen,[(a)] D Baxter,[(b)] LA McCue,[(a)] HJ Sofia,[(a)] BM Webb-Robertson,[(a)] RC Taylor,[(a)] S Havre,[(a)] E Welsh,[(c)] and H Pakrasi[(c)]

(a) Pacific Northwest National Laboratory, Richland, Washington
(b) W.R. Wiley Environmental Molecular Sciences Laboratory, Richland, Washington
(c) Washington University, Saint Louis, Missouri

Cyanobacteria are organisms that are capable of producing energy through photosynthesis and nitrogen fixation. As these organisms represent a large fraction of Earth's total biomass, their energy-producing processes may be a significant source of information related to renewable energy production and environmental cleanup. To fully understand and use these organisms, we modified genetic analysis tools to quickly analyze them at both the genetic and system levels.

Cyanothece is a relatively unstudied cyanobacterium with unique characteristics, including the ability to produce energy through two separate mechanisms: 1) photosynthesis and 2) nitrogen fixation. *Cyanothece* relies on photosynthesis during daylight but "switches" to nitrogen fixation in the absence of light. We might expect this behavior to rely on a "diurnal" cycle, meaning the organism "anticipates" nightfall. However, evidence suggests that circadian cycles play a role in *Cyanothece's* "switching" behavior. Circadian cycles are bio-chemically based processes that react to the change from light to dark. Because switching between nitrogen fixation and photosynthesis requires extensive remodeling of the cell's molecular machinery, we would expect it to be energetically unfavorable, yet *Cyanothece* is a highly efficient organism.

To understand how *Cyanothece* is capable of performing such dramatic changes, we need to understand the underlying genetic mechanisms and how those mechanisms affect the organism at the system level. Using ScalaBLAST and other computational tools, we have been able to rapidly annotate *Cyanothece's* genome. We performed a gene context analysis using Similarity Box software, This analysis led to the discovery of two proteins involved in nitrogen fixation. These discoveries were confirmed in a proteomics study using PQuad (a proteomics results browser), which indicated the differential presence of key nitrogenase proteins from samples taken at night. We used SEBINI (a network inference tool) (Taylor et al. 2006) to infer the relationship of these proteins to other nitrogenase proteins. We also were able to confirm the significance of these proteins at the system level through clustering analysis tools, including metabolomic, proteomic, and microarray analyses. More significantly, the tools we modified and made available through this EMSL Grand Challenge project enabled us to accomplish these analyses in a few minutes. In the past, as similar set of analyses would have taken days. The set of tools used in this study are represented in Figure 1.

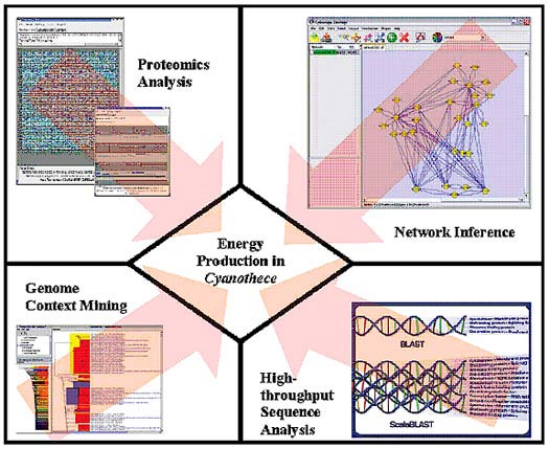

Figure 1. The analysis tools involved in discovery of *Cyanothece's* genetic structure include high-throughput sequence analysis, proteomics analysis, Bayesian network inference, and genome context mining.

Citation

Taylor RC, A Shah, C Treatman, and M Blevins. 2006. "SEBINI: Software Environment for BIological Network Inference." *Bioinformatics* 22(21):2706-2708.

Awards and Recognition

EMSL User Selected to Serve on the Editorial Board for *Laser Chemistry.* WP Hess of PNNL's Fundamental Science Directorate has been selected to serve on the editorial board of the publication *Laser Chemistry*. With his peers on the board, including experts from universities, research foundations, and government councils, Hess will be involved in decisions regarding accepting or rejecting scientific articles submitted for publication in the journal. *Laser Chemistry* is an international journal that focuses on fundamental studies and applications within the field of laser chemical physics and spectroscopy. Hess was selected to serve on the editorial board because of his experience in laser-induced reactions in solids and at surfaces, including his ongoing studies in laser desorption from wide-band gap materials, metal oxides, and semiconductors.

EMSL User Featured in *Battelle World.* A Zelenyuk of PNNL's Fundamental Science Directorate was featured in the May 7, 2007, issue of *Battelle World*. While conducting research at EMSL, Zelenyuk co-invented SPLAT II, which is a second-generation single particle laser ablation time-of-flight mass spectrometer. SPLAT II is a unique, portable instrument that enables scientists to study nanoparticles in both the laboratory and the field. The instrument's particle measurement capabilities provide extremely high sensitivity with unprecedented precision. Combined with a differential mobility analyzer, SPLAT II offers unparalleled details of particles, in real time, by simultaneously measuring shape, size, density, hygroscopicity, fractal dimension, and composition of each individual particle, down to 50 nanometers in diameter. SPLAT analysis can be applied in a wide range of areas including air pollution, climate, human health, bioterrorism, and emerging nanotechnologies.

EMSL Users Featured in *Chemical & Engineering News.* EMSL users A Boldyrev and L-S Wang were featured in the May 7, 2007, issue of *Chemical & Engineering News*. Their computational studies and gas-phase photoelectron spectroscopy experiments confirmed the existence of delocalized bonding involving the d atomic orbitals of transition metals. Research on the planar $Ta_3O_3^-$ cluster provides the first experimental evidence of a δ-aromatic molecule and suggests that δ aromaticity exists in other planar transition-metal complexes.

Professional/Community Service

On April 27, EMSL Director AA Campbell and PNNL user JE Amonette hosted Dr. T Machonkin and several of his undergraduate chemistry students from Whitman College, Walla Walla, Washington. Campbell gave a tour of EMSL and Amonette assisted the students in collecting X-band electron paramagnetic resonance data for a series of transition metal samples in various solvents.

On May 22, laboratory professor J Hylden and students A Guerara, J Benegas, and C Neilsen from Columbia Basin College in Pasco, Washington, toured the EMSL High-Field Magnetic Resonance Facility and ran experiments.

On May 23, EMSL staff member DR Sisk from the EMSL Instrument and Development Laboratory participated in a sumo robot competition at Southridge High School in Kennewick, Washington. The competition was sponsored by Southridge teacher J Hendrick's Engineering Technology Academy in which students learn fundamental engineering through a variety of tasks such as constructing autonomous robots. The annual competition promotes science and engineering education and pits students against technical professionals while providing a fun environment to motivate students to pursue technical fields.

Visitors and Users

During this reporting period, a total of 352 users benefited from EMSL capabilities and expertise. This total included 164 onsite users and 188 remote users.

New EMSL Staff

K Glaesemann recently joined the MSCF staff as a Scientist. Previously, he was at Lawrence Livermore National Laboratory where he oversaw the development of computational chemistry codes, including the thermochemistry program Cheetah. He received his Ph.D. from Iowa State University, where under the supervision of M Gordon he implemented a Grid-Free Density Functional method for GAMESS.

L Larson will be joining the MSCF to replace long-time EMSL employee B Foley, who is retiring. Prior to joining MSCF, Larsen worked for EMSL's Magnetic Resonance and Spectroscopy Group.

Publications

Alary F, J Heully, L Bijeire, and P Vicendo. 2007. "Is the ^{3}MLCT the Only Photoreactive State of Polypyridyl Complexes?" *Inorganic Chemistry* 46(8):3154-3165. DOI: 10.1021/ic062193i.

Chaparadza A, SB Rananavare, and V Shutthanandan. 2007. "Synthesis and Characterization of Lithium-Doped Tin Dioxide Nanocrystalline Powders." *Materials Chemistry and Physics* 102(2-3):176-180. DOI: 10.1016/j.matchemphys.2006.11.022.

Devanathan R and WJ Weber. 2007. "Radiation Effects in a Model Ceramic for Nuclear Waste Disposal." *JOM: Journal of the Minerals, Metals, and Materials Society* 59(4):32-35.

Farber R. 2007. "Will Your Next Supercomputer Come from Costco?" *Scientific Computing* 24(5):13.

Farber R. 2007. "The HPC Brick Wall." *Scientific Computing* 24(6):16.

Farber R. 2007. "Balancing Computation and Experiment." *Innovation: America's Journal of Technology Commercialization* 5(2):24.

Flaherty, DW, Z Dohnálek, A Dohnálkova, BW Arey, DE McCready, N Ponnusamy, CB Mullins, and BD Kay. 2007. "Reactive Ballistic Deposition of Porous TiO_2 Films: Growth and Characterization." *Journal of Physical Chemistry C* 111, 4765-4773.

Jaisi DP, H Dong, and C Liu. 2007. "Kinetic Analysis of Microbial Reduction of Fe(III) in Nontronite." *Environmental Science & Technology* 41(7):2437-2444. DOI: 10.1021/es0619399.

Kamiya M and S Hirata. 2007. "Higher-Order Equation-of-Motion Coupled-Cluster Methods for Electron Attachment." *Journal of Chemical Physics* 126(13): Art.No. 134112. DOI: 10.1063/1.2715575.

Liu G, J Wang, H Wu, Y Lin, and Y Lin. 2007. "Nanovehicles Based Bioassay Labels." *Electroanalysis* 19(7-8):777-785. DOI: 10.1002/élan.200603787.

Migliore A, S Corni, R Di Felice, and E Molinari. 2007. "Water-Mediated Electron Transfer Between Protein Redox Centers." *Journal of Physical Chemistry B* 111(14):3774-3781.

DOI: 10.1021/jp068773i.

Palmer BJ, SM Kathmann, M Krishnan, V Tipparaju, and J Nieplocha. 2007. "The Use of Processor Groups in Molecular Dynamics Simulations to Sample Free-Energy States." *Journal of Chemical Theory and Computation* 3(2):583-592. DOI: 10.1021/ct600260u.

Punnoose A, KM Reddy, A Thurber, J Hays, and MH Engelhard. 2007. "Novel Magnetic Hydrogen Sensing: A Case Study Using Antiferromagnetic Haematite Nanoparticles." *Nanotechnology* 18(16): Art. No. 165502. DOI: 10.1088/0957-4484/18/16/165502.

Saraf LV, MH Engelhard, CM Wang, AS Lea, DE McCready, V Shutthanandan, DR Baer, and SA Chambers. 2007. "Metalorganic Chemical Vapor Deposition of Carbon-Free ZnO Using the Bis (2,2,6,6-tetramethyl-3,5-heptanedionato) Zinc Precursor." *Journal of Materials Research* 22(5):1230-1234. DOI: 10.1557/JMR.2007.0146.

Sendt K and BS Haynes. 2007. "Density Functional Study of the Chemisorption of O-2 across Two Rings of the Armchair Surface of Graphite." *Journal of Physical Chemistry C* 111(14):5465-5473. DOI: 10.1021/jp067363r.

Sun M, Y Ding, G Cui, and Y Liu. 2007. "S-1 and S-2 Excited States of Gas-Phase Schiff-Base Retinal Chromophores: A Time-Dependent Density Functional Theoretical Investigation." *Journal of Physical Chemistry A* 111(15):2946-2950. DOI: 10.1021/jp0709757.

Wang L, S Bulusu, H Zhai, X Zeng, and LS Wang. 2007. "Doping Golden Buckyballs: Cu@Au16- and Cu@Au17- Cluster Anions." *Angewandte Chemie International Edition* 46(16):2915-2918. DOI: 10.1002/anie.200700060.

Wang Z, F Gao, J Crocombette, X Zu, L Yang, and WJ Weber. 2007. "Thermal Conductivity of GaN Nanotubes Simulated by Nonequilibrium Molecular Dynamics." *Physical Review B, Condensed Matter* 75(15): Art. No. 153303. DOI: 10.1103/PhysRevB.75.153303.

Wang Z, X Zu, F Gao, WJ Weber, and J Crocombette. 2007. "Atomistic Simulation of the Size and Orientation Dependences of Thermal Conductivity in GaN Nanowires." *Applied Physics Letters* 90(16): Art. No. 161923. DOI: 10.1063/1.2730747.

Wu H, G Liu, J Wang, and Y Lin. 2007. "Quantum-Dots Based Electrochemical Immunoassay of Interleukin-1α." *Electrochemistry Communications* 9(7):1573-1577. DOI: 10.1016/j.elecom.2007.02.024.

Zhang Q, LV Saraf, and F Hua. 2007. "Transparent Thin-Film Transistor with Self-Assembled Nanocrystals." *Nanotechnology* 18(19): 195204. DOI: 10.1088/0957-4484/18/19/195204.

Zhang W, Y Wang, J Li, J Xue, H Ji, Q Ouyang, J Xu, and Y Zhang. 2007. "Controllable Shrinking and Shaping of Silicon Nitride Nanopores under Electron Irradiation." *Applied Physics Letters* 90(16): Art. No. 163102. DOI: 10.1063/1.2723680.

Presentations

During this reporting period, EMSL staff presented on research performed at the user facility at the following meetings or locations:

- Materials Research Society Spring Meeting, San Francisco, California, April 9, 2007.
- Environmental Remediation Sciences Program Principal Investigator Meeting, Lansdowne, Virginia, April 17, 2007.
- European Geosciences Union General Assembly 2007, Vienna, Austria, April 18-19, 2007.
- Academy of Sciences of the Czech Republic, Prague, Czech Republic, April 24, 2007.
- Separations and Heavy Element Chemistry Contractors' Meeting, Annapolis, Maryland, April 24, 2007.
- HP-Cast Conference, Karlsruhe, Germany, May 6, 2007.
- DOE Biological and Environmental Research Advisory Committee Meeting, Bethesda, Maryland, May 15, 2007.
- Petascale Workshop, San Francisco, California, May 17, 2007.
- Scalable Data Management Special Interest Group, Richland, Washington, May 22, 2007.
- Symposium and Short Course, Solid-State NMR of Metals in Biological Systems and Materials, Newark, Delaware, June 9, 2007.
- Workshop on NMR of Metals in Biological Systems and in Materials, University of Delaware, Newark, Delaware, June 9-10, 2007.

Journal Covers

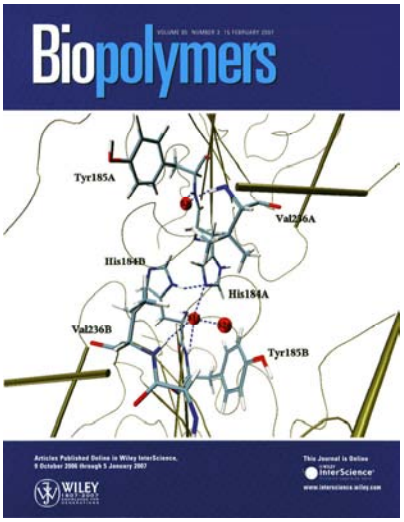

The research of EMSL users C Chen, BW Beck, K Krause, TE Weksberg, and B Montgomery Pettitt was featured on the cover of the February 15, 2007, issue of *Biopolymers*.